

First Observation of the Decay $B_s^0 \rightarrow D_s^- D_s^+$ and Measurement of Its Branching Ratio

CDF Collaboration

CLARK, Allan Geoffrey (Collab.), *et al.*

Abstract

We report the observation of the exclusive decay $B_0s \rightarrow D-sD+s$ at the 7.5 standard deviation level using 355 pb^{-1} of data collected by the CDF II detector in pp collisions at $s\sqrt{=}1.96 \text{ TeV}$ at the Fermilab Tevatron. We measure the relative branching ratio $B(B_0s \rightarrow D-sD+s)/B(B_0 \rightarrow D-D+s) = 1.44 + 0.48 - 0.44$. Using the world average value for $B(B_0 \rightarrow D-D+s)$, we find $B(B_0s \rightarrow D-sD+s) = (9.4 + 4.4 - 4.2) \times 10^{-3}$. This provides a lower bound $\Delta\Gamma_{CPs}/\Gamma_s \geq 2B(B_0s \rightarrow D-sD+s) > 1.2 \times 10^{-2}$ at 95% C.L.

Reference

CDF Collaboration, CLARK, Allan Geoffrey (Collab.), *et al.* First Observation of the Decay $B_s^0 \rightarrow D_s^- D_s^+$ and Measurement of Its Branching Ratio. *Physical Review Letters*, 2008, vol. 100, no. 02, p. 021803

DOI : 10.1103/PhysRevLett.100.021803

Available at:

<http://archive-ouverte.unige.ch/unige:38493>

Disclaimer: layout of this document may differ from the published version.



UNIVERSITÉ
DE GENÈVE

First Observation of the Decay $B_s^0 \rightarrow D_s^- D_s^+$ and Measurement of Its Branching Ratio

T. Aaltonen,²³ J. Adelman,¹³ T. Akimoto,⁵⁴ M. G. Albrow,¹⁷ B. Álvarez González,¹¹ S. Amerio,⁴² D. Amidei,³⁴ A. Anastassov,⁵¹ A. Annovi,¹⁹ J. Antos,¹⁴ M. Aoki,²⁴ G. Apollinari,¹⁷ A. Apresyan,⁴⁷ T. Arisawa,⁵⁶ A. Artikov,¹⁵ W. Ashmanskas,¹⁷ A. Attal,³ A. Aurisano,⁵² F. Azfar,⁴¹ P. Azzi-Bacchetta,⁴² P. Azzurri,⁴⁵ N. Bacchetta,⁴² W. Badgett,¹⁷ A. Barbaro-Galtieri,²⁸ V. E. Barnes,⁴⁷ B. A. Barnett,²⁵ S. Baroiant,⁷ V. Bartsch,³⁰ G. Bauer,³² P.-H. Beauchemin,³³ F. Bedeschi,⁴⁵ P. Bednar,¹⁴ S. Behari,²⁵ G. Bellettini,⁴⁵ J. Bellinger,⁵⁸ A. Belloni,²² D. Benjamin,¹⁶ A. Beretvas,¹⁷ J. Beringer,²⁸ T. Berry,²⁹ A. Bhatti,⁴⁹ M. Binkley,¹⁷ D. Bisello,⁴² I. Bizjak,³⁰ R. E. Blair,² C. Blocker,⁶ B. Blumenfeld,²⁵ A. Bocci,¹⁶ A. Bodek,⁴⁸ V. Boisvert,⁴⁸ G. Bolla,⁴⁷ A. Bolshov,³² D. Bortoletto,⁴⁷ J. Boudreau,⁴⁶ A. Boveia,¹⁰ B. Brau,¹⁰ A. Bridgeman,²⁴ L. Brigliadori,⁵ C. Bromberg,³⁵ E. Brubaker,¹³ J. Budagov,¹⁵ H. S. Budd,⁴⁸ S. Budd,²⁴ K. Burkett,¹⁷ G. Busetto,⁴² P. Bussey,²¹ A. Buzatu,³³ K. L. Byrum,² S. Cabrera,^{16,s} M. Campanelli,³⁵ M. Campbell,³⁴ F. Canelli,¹⁷ A. Canepa,⁴⁴ D. Carlsmith,⁵⁸ R. Carosi,⁴⁵ S. Carrillo,^{18,m} S. Carron,³³ B. Casal,¹¹ M. Casarsa,¹⁷ A. Castro,⁵ P. Catastini,⁴⁵ D. Cauz,⁵³ M. Cavalli-Sforza,³ A. Cerri,²⁸ L. Cerrito,^{30,q} S. H. Chang,²⁷ Y. C. Chen,¹ M. Chertok,⁷ G. Chiarelli,⁴⁵ G. Chlachidze,¹⁷ F. Chlebana,¹⁷ K. Cho,²⁷ D. Chokheli,¹⁵ J. P. Chou,²² G. Choudalakis,³² S. H. Chuang,⁵¹ K. Chung,¹² W. H. Chung,⁵⁸ Y. S. Chung,⁴⁸ C. I. Ciobanu,²⁴ M. A. Ciocci,⁴⁵ A. Clark,²⁰ D. Clark,⁶ G. Compostella,⁴² M. E. Convery,¹⁷ J. Conway,⁷ B. Cooper,³⁰ K. Copic,³⁴ M. Cordelli,¹⁹ G. Cortiana,⁴² F. Crescioli,⁴⁵ C. Cuenca Almenar,^{7,s} J. Cuevas,^{11,p} R. Culbertson,¹⁷ J. C. Cully,³⁴ D. Dagenhart,¹⁷ M. Datta,¹⁷ T. Davies,²¹ P. de Barbaro,⁴⁸ S. De Cecco,⁵⁰ A. Deisher,²⁸ G. De Lentdecker,^{48,e} G. De Lorenzo,³ M. Dell'Orso,⁴⁵ L. Demortier,⁴⁹ J. Deng,¹⁶ M. Deninno,⁵ D. De Pedis,⁵⁰ P. F. Derwent,¹⁷ G. P. Di Giovanni,⁴³ C. Dionisi,⁵⁰ B. Di Ruzza,⁵³ J. R. Dittmann,⁴ M. D'Onofrio,³ S. Donati,⁴⁵ P. Dong,⁸ J. Donini,⁴² T. Dorigo,⁴² S. Dube,⁵¹ J. Efron,³⁸ R. Erbacher,⁷ D. Errede,²⁴ S. Errede,²⁴ R. Eusebi,¹⁷ H. C. Fang,²⁸ S. Farrington,²⁹ W. T. Fedorko,¹³ R. G. Feild,⁵⁹ M. Feindt,²⁶ J. P. Fernandez,³¹ C. Ferrazza,⁴⁵ R. Field,¹⁸ G. Flanagan,⁴⁷ R. Forrest,⁷ S. Forrester,⁷ M. Franklin,²² J. C. Freeman,²⁸ I. Furic,¹⁸ M. Gallinaro,⁴⁹ J. Galyardt,¹² F. Garbersson,¹⁰ J. E. Garcia,⁴⁵ A. F. Garfinkel,⁴⁷ H. Gerberich,²⁴ D. Gerdes,³⁴ S. Giagu,⁵⁰ V. Giakoumopolou,^{45,b} P. Giannetti,⁴⁵ K. Gibson,⁴⁶ J. L. Gimmell,⁴⁸ C. M. Ginsburg,¹⁷ N. Giokaris,^{15,b} M. Giordani,⁵³ P. Giromini,¹⁹ M. Giunta,⁴⁵ V. Glagolev,¹⁵ D. Glenzinski,¹⁷ M. Gold,³⁶ N. Goldschmidt,¹⁸ A. Golossanov,¹⁷ G. Gomez,¹¹ G. Gomez-Ceballos,³² M. Goncharov,⁵² O. González,³¹ I. Gorelov,³⁶ A. T. Goshaw,¹⁶ K. Goulianos,⁴⁹ A. Gresele,⁴² S. Grinstein,²² C. Grosso-Pilcher,¹³ R. C. Group,¹⁷ U. Grundler,²⁴ J. Guimaraes da Costa,²² Z. Gunay-Unalan,³⁵ C. Haber,²⁸ K. Hahn,³² S. R. Hahn,¹⁷ E. Halkiadakis,⁵¹ A. Hamilton,²⁰ B.-Y. Han,⁴⁸ J. Y. Han,⁴⁸ R. Handler,⁵⁸ F. Happacher,¹⁹ K. Hara,⁵⁴ D. Hare,⁵¹ M. Hare,⁵⁵ S. Harper,⁴¹ R. F. Harr,⁵⁷ R. M. Harris,¹⁷ M. Hartz,⁴⁶ K. Hatakeyama,⁴⁹ J. Hauser,⁸ C. Hays,⁴¹ M. Heck,²⁶ A. Heijboer,⁴⁴ B. Heinemann,²⁸ J. Heinrich,⁴⁴ C. Henderson,³² M. Herndon,⁵⁸ J. Heuser,²⁶ S. Hewamanage,⁴ D. Hidas,¹⁶ C. S. Hill,^{10,d} D. Hirschbuehl,²⁶ A. Hocker,¹⁷ S. Hou,¹ M. Houlden,²⁹ S.-C. Hsu,⁹ B. T. Huffman,⁴¹ R. E. Hughes,³⁸ U. Husemann,⁵⁹ J. Huston,³⁵ J. Incandela,¹⁰ G. Introzzi,⁴⁵ M. Iori,⁵⁰ A. Ivanov,⁷ B. Iyutin,³² E. James,¹⁷ B. Jayatilaka,¹⁶ D. Jeans,⁵⁰ E. J. Jeon,²⁷ S. Jindariani,¹⁸ W. Johnson,⁷ M. Jones,⁴⁷ K. K. Joo,²⁷ S. Y. Jun,¹² J. E. Jung,²⁷ T. R. Junk,²⁴ T. Kamon,⁵² D. Kar,¹⁸ P. E. Karchin,⁵⁷ Y. Kato,⁴⁰ R. Kephart,¹⁷ U. Kerzel,²⁶ V. Khotilovich,⁵² B. Kilminster,³⁸ D. H. Kim,²⁷ H. S. Kim,²⁷ J. E. Kim,²⁷ M. J. Kim,¹⁷ S. B. Kim,²⁷ S. H. Kim,⁵⁴ Y. K. Kim,¹³ N. Kimura,⁵⁴ L. Kirsch,⁶ S. Klimentenko,¹⁸ M. Klute,³² B. Knuteson,³² B. R. Ko,¹⁶ S. A. Koay,¹⁰ K. Kondo,⁵⁶ D. J. Kong,²⁷ J. Konigsberg,¹⁸ A. Korytov,¹⁸ A. V. Kotwal,¹⁶ J. Kraus,²⁴ M. Kreps,²⁶ J. Kroll,⁴⁴ N. Krumnack,⁴ M. Kruse,¹⁶ V. Krutelyov,¹⁰ T. Kubo,⁵⁴ S. E. Kuhlmann,² T. Kuhr,²⁶ N. P. Kulkarni,⁵⁷ Y. Kusakabe,⁵⁶ S. Kwang,¹³ A. T. Laasanen,⁴⁷ S. Lai,³³ S. Lami,⁴⁵ S. Lammel,¹⁷ M. Lancaster,³⁰ R. L. Lander,⁷ K. Lannon,³⁸ A. Lath,⁵¹ G. Latino,⁴⁵ I. Lazzizzera,⁴² T. LeCompte,² J. Lee,⁴⁸ J. Lee,²⁷ Y. J. Lee,²⁷ S. W. Lee,^{52,r} R. Lefèvre,²⁰ N. Leonardo,³² S. Leone,⁴⁵ S. Levy,¹³ J. D. Lewis,¹⁷ C. Lin,⁵⁹ C. S. Lin,²⁸ J. Linacre,⁴¹ M. Lindgren,¹⁷ E. Lipeles,⁹ A. Lister,⁷ D. O. Litvintsev,¹⁷ T. Liu,¹⁷ N. S. Lockyer,⁴⁴ A. Loginov,⁵⁹ M. Loreti,⁴² L. Lovas,¹⁴ R.-S. Lu,¹ D. Lucchesi,⁴² J. Lueck,²⁶ C. Luci,⁵⁰ P. Lujan,²⁸ P. Lukens,¹⁷ G. Lungu,¹⁸ L. Lyons,⁴¹ J. Lys,²⁸ R. Lysak,¹⁴ E. Lytken,⁴⁷ P. Mack,²⁶ D. MacQueen,³³ R. Madrak,¹⁷ K. Maeshima,¹⁷ K. Makhoul,³² T. Maki,²³ P. Maksimovic,²⁵ S. Malde,⁴¹ S. Malik,³⁰ G. Manca,²⁹ A. Manousakis,^{15,b} F. Margaroli,⁴⁷ C. Marino,²⁶ C. P. Marino,²⁴ A. Martin,⁵⁹ M. Martin,²⁵ V. Martin,^{21,k} M. Martínez,³ R. Martínez-Ballarín,³¹ T. Maruyama,⁵⁴ P. Mastrandrea,⁵⁰ T. Masubuchi,⁵⁴ M. E. Mattson,⁵⁷ P. Mazzanti,⁵ K. S. McFarland,⁴⁸ P. McIntyre,⁵² R. McNulty,^{29,j} A. Mehta,²⁹ P. Mehtala,²³ S. Menzemer,^{11,l} A. Menzione,⁴⁵ P. Merkel,⁴⁷ C. Mesropian,⁴⁹ A. Messina,³⁵ T. Miao,¹⁷ N. Miladinovic,⁶ J. Miles,³² R. Miller,³⁵ C. Mills,²² M. Milnik,²⁶ A. Mitra,¹ G. Mitselmakher,¹⁸ H. Miyake,⁵⁴ S. Moed,²² N. Moggi,⁵ C. S. Moon,²⁷ R. Moore,¹⁷ M. Morello,⁴⁵ P. Movilla Fernandez,²⁸ J. Mülmenstädt,²⁸ A. Mukherjee,¹⁷ Th. Muller,²⁶ R. Mumford,²⁵ P. Murat,¹⁷ M. Mussini,⁵ J. Nachtman,¹⁷ Y. Nagai,⁵⁴ A. Nagano,⁵⁴ J. Naganoma,⁵⁶ K. Nakamura,⁵⁴

I. Nakano,³⁹ A. Napier,⁵⁵ V. Necula,¹⁶ C. Neu,⁴⁴ M. S. Neubauer,²⁴ J. Nielsen,^{28,g} L. Nodulman,² M. Norman,⁹ O. Norriella,²⁴ E. Nurse,³⁰ S. H. Oh,¹⁶ Y. D. Oh,²⁷ I. Oksuzian,¹⁸ T. Okusawa,⁴⁰ R. Oldeman,²⁹ R. Orava,²³ K. Osterberg,³³ S. Pagan Griso,⁴² C. Pagliarone,⁴⁵ E. Palencia,¹⁷ V. Papadimitriou,¹⁷ A. Papaikononou,²⁶ A. A. Paramonov,¹³ B. Parks,³⁸ S. Pashapour,³³ J. Patrick,¹⁷ G. Pauletta,⁵³ M. Paulini,¹² C. Paus,³² D. E. Pellett,⁷ A. Penzo,⁵³ T. J. Phillips,¹⁶ G. Piacentino,⁴⁵ J. Piedra,⁴³ L. Pinares,¹⁸ K. Pitts,²⁴ C. Plager,⁸ L. Pondrom,⁵⁸ X. Portell,³ O. Poukhov,¹⁵ N. Pounder,⁴¹ F. Prakoshyn,¹⁵ A. Pronko,¹⁷ J. Proudfoot,² F. Ptohos,^{17,i} G. Punzi,⁴⁵ J. Pursley,⁵⁸ J. Rademacker,^{41,d} A. Rahaman,⁴⁶ V. Ramakrishnan,⁵⁸ N. Ranjan,⁴⁷ I. Redondo,³¹ B. Reisert,¹⁷ V. Rekovic,³⁶ P. Renton,⁴¹ M. Rescigno,⁵⁰ S. Richter,²⁶ F. Rimondi,⁵ L. Ristori,⁴⁵ A. Robson,²¹ T. Rodrigo,¹¹ E. Rogers,²⁴ S. Rolli,⁵⁵ R. Roser,¹⁷ M. Rossi,⁵³ R. Rossin,¹⁰ P. Roy,³³ A. Ruiz,¹¹ J. Russ,¹² V. Rusu,¹⁷ H. Saarikko,²³ A. Safonov,⁵² W. K. Sakumoto,⁴⁸ G. Salamanna,⁵⁰ O. Saltó,³ L. Santi,⁵³ S. Sarkar,⁵⁰ L. Sartori,⁴⁵ K. Sato,¹⁷ A. Savoy-Navarro,⁴³ T. Scheidle,²⁶ P. Schlabach,¹⁷ E. E. Schmidt,¹⁷ M. A. Schmidt,¹³ M. P. Schmidt,⁵⁹ M. Schmitt,³⁷ T. Schwarz,⁷ L. Scodellaro,¹¹ A. L. Scott,¹⁰ A. Scribano,⁴⁵ F. Scuri,⁴⁵ A. Sedov,⁴⁷ S. Seidel,³⁶ Y. Seiya,⁴⁰ A. Semenov,¹⁵ L. Sexton-Kennedy,¹⁷ A. Sfyria,²⁰ S. Z. Shalhout,⁵⁷ M. D. Shapiro,²⁸ T. Shears,²⁹ P. F. Shepard,⁴⁶ D. Sherman,²² M. Shimojima,^{54,o} M. Shochet,¹³ Y. Shon,⁵⁸ I. Shreyber,²⁰ A. Sidoti,⁴⁵ P. Sinervo,³³ A. Sisakyan,¹⁵ A. J. Slaughter,¹⁷ J. Slaunwhite,³⁸ K. Sliwa,⁵⁵ J. R. Smith,⁷ F. D. Snider,¹⁷ R. Snihur,³³ M. Soderberg,³⁴ A. Soha,⁷ S. Somalwar,⁵¹ V. Sorin,³⁵ J. Spalding,¹⁷ F. Spinella,⁴⁵ T. Spreitzer,³³ P. Squillacioti,⁴⁵ M. Stanitzki,⁵⁹ R. St. Denis,²¹ B. Stelzer,⁸ O. Stelzer-Chilton,⁴¹ D. Stentz,³⁷ J. Strologas,³⁶ D. Stuart,¹⁰ J. S. Suh,²⁷ A. Sukhanov,¹⁸ H. Sun,⁵⁵ I. Suslov,¹⁵ T. Suzuki,⁵⁴ A. Taffard,^{24,f} R. Takashima,³⁹ Y. Takeuchi,⁵⁴ R. Tanaka,³⁹ M. Tecchio,³⁴ P. K. Teng,¹ K. Terashi,⁴⁹ J. Thom,^{17,h} A. S. Thompson,²¹ G. A. Thompson,²⁴ E. Thomson,⁴⁴ P. Tipton,⁵⁹ V. Tiwari,¹² S. Tkaczyk,¹⁷ D. Toback,⁵² S. Tokar,¹⁴ K. Tollefson,³⁵ T. Tomura,⁵⁴ D. Tonelli,¹⁷ S. Torre,¹⁹ D. Torretta,¹⁷ S. Tourneur,⁴³ W. Trischuk,³³ Y. Tu,⁴⁴ N. Turini,⁴⁵ F. Ukegawa,⁵⁴ S. Uozumi,⁵⁴ S. Vallecorsa,²⁰ N. van Remortel,²³ A. Varganov,³⁴ E. Vataga,³⁶ F. Vázquez,^{18,m} G. Velev,¹⁷ C. Vellidis,^{45,b} V. Veszpremi,⁴⁷ M. Vidal,³¹ R. Vidal,¹⁷ I. Vila,¹¹ R. Vilar,¹¹ T. Vine,³⁰ M. Vogel,³⁶ I. Volobouev,^{28,r} G. Volpi,⁴⁵ F. Würthwein,⁹ P. Wagner,⁴⁴ R. G. Wagner,² R. L. Wagner,¹⁷ J. Wagner-Kuhr,²⁶ W. Wagner,²⁶ T. Wakisaka,⁴⁰ R. Wallny,⁸ S. M. Wang,¹ A. Warburton,³³ D. Waters,³⁰ M. Weinberger,⁵² W. C. Wester III,¹⁷ B. Whitehouse,⁵⁵ D. Whiteson,^{44,f} A. B. Wicklund,² E. Wicklund,¹⁷ G. Williams,³³ H. H. Williams,⁴⁴ P. Wilson,¹⁷ B. L. Winer,³⁸ P. Wittich,^{17,h} S. Wolbers,¹⁷ C. Wolfe,¹³ T. Wright,³⁴ X. Wu,²⁰ S. M. Wynne,²⁹ A. Yagil,⁹ K. Yamamoto,⁴⁰ J. Yamaoka,⁵¹ T. Yamashita,³⁹ C. Yang,⁵⁹ U. K. Yang,^{13,n} Y. C. Yang,²⁷ W. M. Yao,²⁸ G. P. Yeh,¹⁷ J. Yoh,¹⁷ K. Yorita,¹³ T. Yoshida,⁴⁰ G. B. Yu,⁴⁸ I. Yu,²⁷ S. S. Yu,¹⁷ J. C. Yun,¹⁷ L. Zanello,⁵⁰ A. Zanetti,⁵³ I. Zaw,²² X. Zhang,²⁴ Y. Zheng,^{8,c} and S. Zucchelli⁵

(CDF Collaboration)^a¹*Institute of Physics, Academia Sinica, Taipei, Taiwan 11529, People's Republic of China*²*Argonne National Laboratory, Argonne, Illinois 60439, USA*³*Institut de Física d'Altes Energies, Universitat Autònoma de Barcelona, E-08193, Bellaterra (Barcelona), Spain*⁴*Baylor University, Waco, Texas 76798, USA*⁵*Istituto Nazionale di Fisica Nucleare, University of Bologna, I-40127 Bologna, Italy*⁶*Brandeis University, Waltham, Massachusetts 02254, USA*⁷*University of California, Davis, Davis, California 95616, USA*⁸*University of California, Los Angeles, Los Angeles, California 90024, USA*⁹*University of California, San Diego, La Jolla, California 92093, USA*¹⁰*University of California, Santa Barbara, Santa Barbara, California 93106, USA*¹¹*Instituto de Física de Cantabria, CSIC-University of Cantabria, 39005 Santander, Spain*¹²*Carnegie Mellon University, Pittsburgh, Pennsylvania 15213, USA*¹³*Enrico Fermi Institute, University of Chicago, Chicago, Illinois 60637, USA*¹⁴*Comenius University, 842 48 Bratislava, Slovakia and Institute of Experimental Physics, 040 01 Kosice, Slovakia*¹⁵*Joint Institute for Nuclear Research, RU-141980 Dubna, Russia*¹⁶*Duke University, Durham, North Carolina 27708, USA*¹⁷*Fermi National Accelerator Laboratory, Batavia, Illinois 60510, USA*¹⁸*University of Florida, Gainesville, Florida 32611, USA*¹⁹*Laboratori Nazionali di Frascati, Istituto Nazionale di Fisica Nucleare, I-00044 Frascati, Italy*²⁰*University of Geneva, CH-1211 Geneva 4, Switzerland*²¹*Glasgow University, Glasgow G12 8QQ, United Kingdom*²²*Harvard University, Cambridge, Massachusetts 02138, USA*²³*Division of High Energy Physics, Department of Physics, University of Helsinki and Helsinki Institute of Physics, FIN-00014, Helsinki, Finland*

- ²⁴University of Illinois, Urbana, Illinois 61801, USA
²⁵The Johns Hopkins University, Baltimore, Maryland 21218, USA
²⁶Institut für Experimentelle Kernphysik, Universität Karlsruhe, 76128 Karlsruhe, Germany
²⁷Center for High Energy Physics: Kyungpook National University, Daegu 702-701, Korea;
 Seoul National University, Seoul 151-742, Korea;
 Sungkyunkwan University, Suwon 440-746, Korea;
 Korea Institute of Science and Technology Information, Daejeon, 305-806, Korea;
 Chonnam National University, Gwangju, 500-757, Korea
²⁸Ernest Orlando Lawrence Berkeley National Laboratory, Berkeley, California 94720, USA
²⁹University of Liverpool, Liverpool L69 7ZE, United Kingdom
³⁰University College London, London WC1E 6BT, United Kingdom
³¹Centro de Investigaciones Energeticas Medioambientales y Tecnológicas, E-28040 Madrid, Spain
³²Massachusetts Institute of Technology, Cambridge, Massachusetts 02139, USA
³³Institute of Particle Physics: McGill University, Montréal, Canada H3A 2T8;
 and University of Toronto, Toronto, Canada M5S 1A7
³⁴University of Michigan, Ann Arbor, Michigan 48109, USA
³⁵Michigan State University, East Lansing, Michigan 48824, USA
³⁶University of New Mexico, Albuquerque, New Mexico 87131, USA
³⁷Northwestern University, Evanston, Illinois 60208, USA
³⁸The Ohio State University, Columbus, Ohio 43210, USA
³⁹Okayama University, Okayama 700-8530, Japan
⁴⁰Osaka City University, Osaka 588, Japan
⁴¹University of Oxford, Oxford OX1 3RH, United Kingdom
⁴²Istituto Nazionale di Fisica Nucleare, University of Padova, Sezione di Padova-Trento, I-35131 Padova, Italy
⁴³LPNHE, Université Pierre et Marie Curie/IN2P3-CNRS, UMR7585, Paris, F-75252 France
⁴⁴University of Pennsylvania, Philadelphia, Pennsylvania 19104, USA
⁴⁵Istituto Nazionale di Fisica Nucleare Pisa, University of Pisa, University of Siena, and Scuola Normale Superiore,
 I-56127 Pisa, Italy
⁴⁶University of Pittsburgh, Pittsburgh, Pennsylvania 15260, USA
⁴⁷Purdue University, West Lafayette, Indiana 47907, USA
⁴⁸University of Rochester, Rochester, New York 14627, USA
⁴⁹The Rockefeller University, New York, New York 10021, USA
⁵⁰Istituto Nazionale di Fisica Nucleare, Sezione di Roma 1, University of Rome “La Sapienza,” I-00185 Roma, Italy
⁵¹Rutgers University, Piscataway, New Jersey 08855, USA
⁵²Texas A&M University, College Station, Texas 77843, USA
⁵³Istituto Nazionale di Fisica Nucleare, University of Trieste/Udine, Italy
⁵⁴University of Tsukuba, Tsukuba, Ibaraki 305, Japan
⁵⁵Tufts University, Medford, Massachusetts 02155, USA
⁵⁶Waseda University, Tokyo 169, Japan
⁵⁷Wayne State University, Detroit, Michigan 48201, USA
⁵⁸University of Wisconsin, Madison, Wisconsin 53706, USA
⁵⁹Yale University, New Haven, Connecticut 06520, USA
 (Received 25 July 2007; published 16 January 2008)

We report the observation of the exclusive decay $B_s^0 \rightarrow D_s^- D_s^+$ at the 7.5 standard deviation level using 355 pb^{-1} of data collected by the CDF II detector in $p\bar{p}$ collisions at $\sqrt{s} = 1.96 \text{ TeV}$ at the Fermilab Tevatron. We measure the relative branching ratio $\mathcal{B}(B_s^0 \rightarrow D_s^- D_s^+)/\mathcal{B}(B^0 \rightarrow D^- D_s^+) = 1.44_{-0.44}^{+0.48}$. Using the world average value for $\mathcal{B}(B^0 \rightarrow D^- D_s^+)$, we find $\mathcal{B}(B_s^0 \rightarrow D_s^- D_s^+) = (9.4_{-4.2}^{+4.4}) \times 10^{-3}$. This provides a lower bound $\Delta\Gamma_s^{CP}/\Gamma_s \geq 2\mathcal{B}(B_s^0 \rightarrow D_s^- D_s^+) > 1.2 \times 10^{-2}$ at 95% C.L.

DOI: 10.1103/PhysRevLett.100.021803

PACS numbers: 13.25.Hw, 14.40.Nd

The $B_s^0 - \bar{B}_s^0$ system exhibits mixing, with two distinct mass eigenstates B_H and B_L having a mass difference $\Delta m_s = m_s^H - m_s^L$, which has recently been measured [1]. In the standard model, these two states have decay widths Γ_s^L and Γ_s^H , with difference $\Delta\Gamma_s = \Gamma_s^L - \Gamma_s^H$ and average $\Gamma_s = (\Gamma_s^L + \Gamma_s^H)/2$. To good approximation, the two mass eigenstates are expected to be eigenstates of CP : B_s^{even} and B_s^{odd} , so that $\Delta\Gamma_s \approx \Delta\Gamma_s^{CP}$, where $\Delta\Gamma_s^{CP} = \Gamma(B_s^{\text{even}}) -$

$\Gamma(B_s^{\text{odd}})$. The Standard Model predicts $\Delta\Gamma_s/\Gamma_s = 0.147 \pm 0.060$ [2] with a reasonably small uncertainty. A measurement of this quantity can therefore provide a sensitive test and in case of a discrepancy it would be a good indicator for new physics. Measuring the B_s^0 decay rate to $D_s^{(*)-} D_s^{(*)+}$, where $D_s^{(*)\pm}$ stands for either D_s^\pm or $D_s^{*\pm}$, determines $\Delta\Gamma_s^{CP}/\Gamma_s$, assuming the $b \rightarrow c\bar{c}s$ transitions are dominated by these decays, and neglecting small

CP -odd components [3]:

$$\frac{\Delta\Gamma_s^{CP}}{\Gamma_s} = 2\mathcal{B}(B_s^0 \rightarrow D_s^{(*)-} D_s^{(*)+}). \quad (1)$$

The inclusive measurement of the $B_s^0 \rightarrow D_s^{(*)-} D_s^{(*)+}$ decay rate has been reported previously [4] using $B_s^0 \rightarrow \phi\phi X$ correlations. In this Letter we present the first observation of the exclusive decay $B_s^0 \rightarrow D_s^- D_s^+$ [5], measure the ratio of its branching fraction with respect to that for $B^0 \rightarrow D^- D_s^+$, and set a lower bound on $\Delta\Gamma_s^{CP}/\Gamma_s$. We use CDF II detector data corresponding to 355 pb^{-1} of integrated luminosity of $p\bar{p}$ collisions at $\sqrt{s} = 1.96 \text{ TeV}$ at the Fermilab Tevatron [6].

This analysis depends primarily on the charged particle tracking systems. Charged particle tracks are reconstructed using the hits in the silicon microstrip detector system and the central outer tracker (COT) in the pseudorapidity range $|\eta| \leq 1.0$, where η is defined as $-\ln \tan(\theta/2)$ and θ represents the angle between the particle and the proton beam direction [7]. Both detectors are inside a 1.4 T uniform magnetic field. The silicon detector is composed of L00 (single layer of silicon microstrip sensors close to the beam pipe), the silicon vertex detector (SVX II) (five cylindrical layers of double-sided sensors), and intermediate silicon layers, providing up to 8 coordinate measurements in the r - ϕ view [8]. Surrounding the SVX is the COT, a cylindrical drift chamber with 96 layers of sense wires [9].

A sample rich in charm and beauty hadrons is selected by a three-level displaced track trigger. At level 1, tracks are reconstructed in the COT by the track trigger processor (Extremely Fast Tracker, XFT) [10]. The trigger requires two tracks with transverse momenta $p_T > 2 \text{ GeV}/c$ and the scalar sum $p_{T1} + p_{T2} > 4.0 \text{ GeV}/c$. The level 2 silicon vertex trigger [11] associates SVX II r - ϕ position measurements with Extremely Fast Tracker tracks and provides a precise measurement of the track impact parameter (d_0), the distance of closest approach of the track helix to the beam axis in the transverse plane. Decays of heavy flavor particles are identified by requiring two tracks with $0.12 \text{ mm} \leq d_0 \leq 1 \text{ mm}$ and an opening angle in the transverse plane $2^\circ \leq |\Delta\phi| \leq 90^\circ$. A requirement $L_{xy} > 0.2 \text{ mm}$ is also applied, where L_{xy} is defined as the distance in the transverse plane from the beam line to the two-track vertex projected onto the two-track momentum vector. The level 3 trigger applies the level 1 and level 2 selection requirements after a full event reconstruction.

We measure the branching fraction ratio $\mathcal{B}(B_s^0 \rightarrow D_s^- D_s^+)/\mathcal{B}(B^0 \rightarrow D^- D_s^+)$ in which the D_s^+ meson decay rates and part of the systematic uncertainties cancel. In searching for $B_s^0 \rightarrow D_s^- D_s^+$ we require the decay $D_s^- \rightarrow \phi\pi^-$. To enhance the search sensitivity we reconstruct D_s^+ meson candidates in the $\phi\pi^+$, $\bar{K}^{*0}K^+$, or $\pi^+\pi^+\pi^-$ decay channels for both the B^0 and B_s^0 signals. The ratio is measured independently for three D_s^+ decay modes and is calculated using

$$\frac{\mathcal{B}(B_s^0 \rightarrow D_s^- D_s^+)}{\mathcal{B}(B^0 \rightarrow D^- D_s^+)} = \frac{N_{B_s^0} \epsilon_{B_s^0} f_d}{N_{B^0} \epsilon_{B^0} f_s} \frac{\mathcal{B}(D^- \rightarrow K^+ \pi^- \pi^-)}{\mathcal{B}(D_s^- \rightarrow \phi\pi^-)}, \quad (2)$$

where $N_{B_s^0}$ and N_{B^0} are the measured signal yields, $\epsilon_{B_s^0}/\epsilon_{B^0}$ is the ratio of reconstruction and trigger efficiencies extracted from Monte Carlo simulation, f_s/f_d is the ratio of b quark fragmentation fractions into B_s^0 and B^0 mesons, and $\mathcal{B}(D^- \rightarrow K^+ \pi^- \pi^-)/\mathcal{B}(D_s^- \rightarrow \phi\pi^-)$ is the ratio of branching fractions determined by other experiments.

All tracks used in reconstruction must have $p_T > 350 \text{ MeV}/c$ and are assumed to be either pions or kaons depending on the specific reconstruction hypothesis. The reconstruction of $B^0 \rightarrow D^-(K^+ \pi^- \pi^-)D_s^+(\phi\pi^+)$, for example, begins by searching for $D_s^+ \rightarrow \phi\pi^+$ candidates. We require two oppositely charged tracks to form $\phi \rightarrow K^+K^-$ and then add a third track to form $D_s^+ \rightarrow \phi\pi^+$. The reconstruction of D^- mesons uses the $D^- \rightarrow K^+ \pi^- \pi^-$ mode. We reconstruct $B^0 \rightarrow D^- D_s^+$ candidates by applying a fit to six tracks with constraints on a primary B meson decay vertex, two secondary D meson decay vertices, and the masses of the D mesons.

Monte Carlo simulations are used to optimize the selection requirements, to derive fitting functions for signal and background, and to determine the trigger and reconstruction efficiencies. Single B hadrons are generated without fragmentation products of underlying event particles, and their decays are simulated using EVTGEN [12]. The detector response, including the trigger, is modeled using the CDF simulation package [13]. The selection requirements are optimized by maximizing the significance of the Monte Carlo simulated signal, scaled to the expected yield, relative to the combinatorial background using a method valid for low statistics [14]. Combinatorial background is fitted in the interval $[5.4, 6.0] \text{ GeV}/c^2$ and extrapolated into a $60 \text{ MeV}/c^2$ wide signal region centered around the appropriate B meson mass. Selection requirements are made on the minimum p_T of the tracks, the impact parameter of the B meson, and the χ^2 masses of ϕ and K^{*0} candidates. We also make requirements on the significance of the L_{xy} measurement, $L_{xy}/\sigma(L_{xy})$, where $\sigma(L_{xy})$ is the L_{xy} uncertainty, of B and D meson vertices, and of the displacement of the D meson vertices with respect to the B meson vertex. For decays involving resonant states, we require $1010 \text{ MeV}/c^2 < m(K^+K^-) < 1029 \text{ MeV}/c^2$ for ϕ candidates and $840 \text{ MeV}/c^2 < m(K^- \pi^+) < 940 \text{ MeV}/c^2$ for K^{*0} candidates. The background from $\bar{B}^0 \rightarrow D^+(K^- \pi^+ \pi^+)D_s^-(\phi\pi^-)$ is removed from the $B_s^0 \rightarrow D_s^-(\phi\pi^-)D_s^+(\bar{K}^{*0}K^+)$ signal by reconstructing $D_s^+ \rightarrow \bar{K}^{*0}K^+$ as $D^+ \rightarrow K^- \pi^+ \pi^+$ and removing events with the D^+ candidate mass in the range $1845 \text{ MeV}/c^2 < m(K^- \pi^+ \pi^+) < 1893 \text{ MeV}/c^2$.

Figure 1 shows the reconstructed mass spectra for $B_s^0 \rightarrow D_s^- D_s^+$ and $B^0 \rightarrow D^- D_s^+$ decays. The signal yields $N_{B_s^0}$ and N_{B^0} are extracted from a binned likelihood fit of these

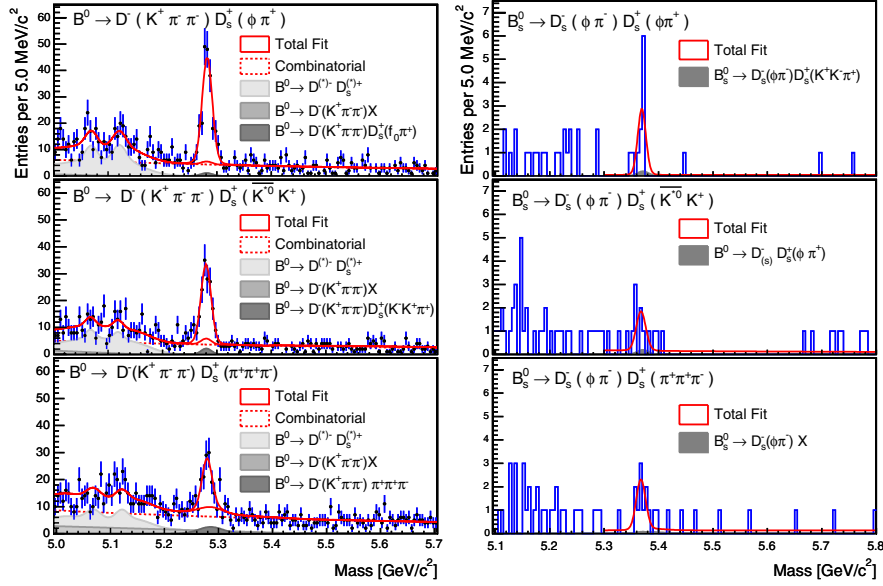


FIG. 1 (color online). Mass spectra for $B^0 \rightarrow D^- D_s^+$ (left) and $B_s^0 \rightarrow D_s^- D_s^+$ (right) where $D_s^+ \rightarrow \phi \pi^+$ (top), $D_s^+ \rightarrow \bar{K}^{*0} K^+$ (middle), $D_s^+ \rightarrow \pi^+ \pi^+ \pi^-$ (bottom). The decomposition of the background into combinatorial background and several backgrounds from B hadron decays is shown. For B^0 decays data are represented with dots and error bars, while for the small event yield B_s^0 channels a histogram is shown.

spectra. The fitting functions for all the modes have terms describing the signal, combinatorial background, partially reconstructed B hadrons, and contributions from B decays to different D_s^+ decay modes. The combinatorial background is represented by the sum of a constant plus an exponential. The signal and partially reconstructed modes are fitted with templates that have fixed shapes derived from simulation and floating normalizations. Each signal template is parametrized by two Gaussians with different widths and a common mean.

In fitting $B_s^0 \rightarrow D_s^- D_s^+$ distributions, we fix the signal masses to Particle Data Group values [15], and we fix the Gaussian signal widths, dominated by detector resolution, to the values obtained from Monte Carlo simulation. We also limit the mass range in the fit to value above 5.3 GeV/c^2 avoiding a detailed description of the well separated physics background.

We treat the background from the decay mode $B^0 \rightarrow D^- \pi^+ \pi^+ \pi^-$ to the signal for $B^0 \rightarrow D^-(K^+ \pi^- \pi^-) \times$

$D_s^+(\bar{K}^{*0} K^+)$ and $B^0 \rightarrow D^-(K^+ \pi^- \pi^-) D_s^+(\pi^+ \pi^+ \pi^-)$ modes by introducing templates normalized to the B^0 yield. Similarly, we introduce the template normalized to the B_s^0 yield to model $B_s^0 \rightarrow D_s^-(\phi \pi^-) \pi^+ \pi^+ \pi^-$ background under the signal for $B_s^0 \rightarrow D_s^-(\phi \pi^-) \times D_s^+(\pi^+ \pi^+ \pi^-)$ mode. These corrections lead to a less than 2% change in the signal.

Monte Carlo studies show that a B meson signal, reconstructed in a specific D_s^+ decay mode, have contributions from misreconstructed B meson candidates decaying through other D_s channels. The decay $B^0 \rightarrow D^- D_s^+$, followed by $D_s^+ \rightarrow f_0(980)(K^+ K^-) \pi^+$, contributes to the reconstructed $B^0 \rightarrow D^-(K^+ \pi^- \pi^-) D_s^+(\phi \pi^+)$. Similarly, B meson decays followed by a nonresonant $D_s^+ \rightarrow K^+ K^- \pi^+$ contribute to the B meson signal reconstructed with $D_s^+ \rightarrow \bar{K}^{*0} K^+$. The $D_s^+ \rightarrow K^+ K^- \pi^+$ decay model takes into account the measured branching fractions of its resonant substructure [16]. The aforementioned effects are taken into account by introducing correction templates

TABLE I. Summary of event yields, efficiencies, measured ratios of branching fractions, and corresponding uncertainties for three D_s^+ decay modes.

	$\phi \pi^+$	$\bar{K}^{*0} K^+$	$\pi^+ \pi^+ \pi^-$
$N(B^0 \rightarrow D^- D_s^+)$	183 ± 15	128 ± 13	84 ± 13
$N(B_s^0 \rightarrow D_s^- D_s^+)$	$9.2_{-2.9}^{+3.5}$	$6.0_{-2.7}^{+3.4}$	$8.3_{-2.8}^{+3.5}$
$\epsilon(B_s^0 \rightarrow D_s^- D_s^+)/\epsilon(B^0 \rightarrow D^- D_s^+)$	0.88 ± 0.03	0.53 ± 0.02	0.63 ± 0.02
$\mathcal{B}(B_s^0 \rightarrow D_s^- D_s^+)/\mathcal{B}(B^0 \rightarrow D^- D_s^+)$	$0.98_{-0.32}^{+0.38}$	$1.51_{-0.70}^{+0.87}$	$2.67_{-0.99}^{+1.20}$
systematic uncertainty	$+0.06/-0.08$	$+0.15/-0.25$	$+0.27/-0.29$
(f_s/f_d) uncertainty	± 0.14	± 0.22	± 0.39
$\mathcal{B}(D_s^- \rightarrow \phi \pi^-)/\mathcal{B}(D^- \rightarrow K^+ \pi^- \pi^-)$ uncertainty	± 0.13	± 0.20	± 0.36

TABLE II. Systematic uncertainties in [%] for the B_s^0/B^0 relative branching fraction measurements for three D_s^+ decay modes.

	$\phi\pi^+$	$\bar{K}^{*0}K^+$	$\pi^+\pi^+\pi^-$
$B^0 \rightarrow D^- D_s^+$ fit	± 2.3	± 4.2	± 8.4
$B_s^0 \rightarrow D_s^- D_s^+$ fit	± 4.4	± 8.2	± 4.6
B meson p_T spectrum	± 3.0	± 3.0	± 3.0
B_s^0 lifetime	± 2.0	± 2.0	± 2.0
trigger	± 1.0	± 1.0	± 1.0
$D_s^+ \rightarrow \pi^+\pi^+\pi^-$ composition	-	-	± 3.0
optimization bias	-5.0	-13.0	-4.0
Total	$+6.2$ -8.0	$+9.9$ -16.4	$+10.3$ -11.0

with relative normalizations derived from Monte Carlo simulations and result in a 4% correction to the signal yield. Other b hadron backgrounds are described with templates derived from semigeneric simulations ($B \rightarrow D_{(s)}^- X$), where one of the $D_{(s)}^-$ mesons is forced to decay in the signal channel and the rest of the decay chain (X) follows the best available measurement of branching fractions.

Yields and ratios of reconstruction efficiencies extracted from signal simulations are summarized in Table I. Using Eq. (2) and the latest PDG [15] values $f_s/f_d = 0.259 \pm 0.038$, and $\mathcal{B}(D_s^- \rightarrow \phi\pi^-) \times \mathcal{B}(\phi \rightarrow K^+K^-) = (2.16 \pm 0.28) \times 10^{-2}$, we calculate the ratio of branching fractions $\mathcal{B}(B_s^0 \rightarrow D_s^- D_s^+)/\mathcal{B}(B^0 \rightarrow D^- D_s^+)$ for the three D_s^+ modes shown in Table I along with corresponding statistical uncertainties, systematic uncertainties discussed below, and the uncertainties from the measurements of f_s/f_d and $\mathcal{B}(D_s^- \rightarrow \phi\pi^-)/\mathcal{B}(D^- \rightarrow K^+\pi^-\pi^-)$.

The systematic uncertainties, summarized in Table II, are evaluated from the change in the ratio of the branching fractions $\mathcal{B}(B_s^0 \rightarrow D_s^- D_s^+)/\mathcal{B}(B^0 \rightarrow D^- D_s^+)$ for each effect under consideration. Fit systematic uncertainties are estimated by varying the fit window, binning, and template parameters. The normalizations of background templates underneath the signal peaks are varied using the measured branching fractions [15] within their uncertainties and the effect is included in the fit systematics in Table II. The uncertainty due to the B meson p_T spectrum is evaluated by comparing the efficiency determined from simulation based on next-to-leading-order calculations [17] and on the measured B hadron spectrum [18]. The effect of meson lifetimes is studied by varying the world average B_s^0 and B^0 lifetimes within their uncertainties in the simulations. Trigger-related systematic uncertainties are estimated from simulations. The effects due to the limited knowledge of the $D_s^+ \rightarrow \pi^+\pi^+\pi^-$ composition are studied by varying the relative branching fractions of the components of the decay within their PDG [15] uncertainties. Finally, using the combinatorial background from data to optimize the selection introduces a bias. This effect has been esti-

mated using simulation based on the expected combinatorial background distribution.

The significance of the $B_s^0 \rightarrow D_s^- D_s^+$ signal is given by the ratio of likelihoods of the mass fits, where we use the one of full fit model divided by the one of the same model but excluding the signal component. The individual significances of the signal reconstructed with $B_s^0 \rightarrow D_s^- (\phi\pi^-) D_s^+ (\phi\pi^+)$, $B_s^0 \rightarrow D_s^- (\phi\pi^-) D_s^+ (\bar{K}^{*0}K^+)$, and $B_s^0 \rightarrow D_s^- (\phi\pi^-) D_s^+ (\pi^+\pi^+\pi^-)$ decay modes are 5.8σ , 3.4σ , and 4.4σ , respectively. From the product of three likelihoods we find the combined result consistent with an observation of $B_s^0 \rightarrow D_s^- D_s^+$ at a 7.5σ significance.

When combining the three results, the fit systematic uncertainties are weighed by the measured yields. The rest of the systematic uncertainties, except for the $D_s^+ \rightarrow \pi^+\pi^+\pi^-$ composition uncertainty, are considered common for all three modes. We find

$$\frac{\mathcal{B}(B_s^0 \rightarrow D_s^- D_s^+)}{\mathcal{B}(B^0 \rightarrow D^- D_s^+)} = 1.44_{-0.31}^{+0.38}(\text{stat})_{-0.12}^{+0.08}(\text{syst}) \pm 0.21(f_s/f_d) \pm 0.20\left(\frac{\mathcal{B}(D^- \rightarrow K^+\pi^-\pi^-)}{\mathcal{B}(D_s^- \rightarrow \phi\pi^-)}\right), \quad (3)$$

which we combine with $\mathcal{B}(B^0 \rightarrow D^- D_s^+) = (6.5 \pm 2.1) \times 10^{-3}$ [15] and determine

$$\mathcal{B}(B_s^0 \rightarrow D_s^- D_s^+) = (9.4_{-4.2}^{+4.4}) \times 10^{-3}, \quad (4)$$

from which we derive a lower limit on $\Delta\Gamma_s^{CP}/\Gamma$:

$$\frac{\Delta\Gamma_s^{CP}}{\Gamma_s} = 2\mathcal{B}(B_s^0 \rightarrow D_s^{(*)-} D_s^{(*)+}) \geq 2\mathcal{B}(B_s^0 \rightarrow D_s^- D_s^+) \geq 1.2 \times 10^{-2} \quad \text{at } 95\% \text{ C.L.} \quad (5)$$

In the derivation of the lower limit we take into account the Poisson statistical fluctuations of the signal yields and the Gaussian distribution for systematics uncertainties.

We have presented the first observation of the decay $B_s^0 \rightarrow D_s^- D_s^+$ and have measured its branching fraction with respect to $B^0 \rightarrow D^- D_s^+$. We set a lower bound on $\Delta\Gamma_s^{CP}/\Gamma_s$, which at the 95% confidence level requires a nonzero decay rate difference and agrees with theoretical predictions [2] and other experimental data: $-0.06 < \Delta\Gamma_s/\Gamma_s < 0.28$ at the 95% confidence level [15].

We thank the Fermilab staff and the technical staffs of the participating institutions for their vital contributions. This work was supported by the U.S. Department of Energy and National Science Foundation; the Italian Istituto Nazionale di Fisica Nucleare; the Ministry of Education, Culture, Sports, Science, and Technology of Japan; the Natural Sciences and Engineering Research Council of Canada; the National Science Council of the Republic of China; the Swiss National Science Foundation; the A.P. Sloan Foundation; the Bundes-

ministerium für Bildung und Forschung, Germany; the Korean Science and Engineering Foundation and the Korean Research Foundation; the Particle Physics and Astronomy Research Council and the Royal Society, United Kingdom; the Russian Foundation for Basic Research; the Comisión Interministerial de Ciencia y Tecnología, Spain; in part by the European Community's Human Potential Programme under Contract No. HPRN-CT-2002-00292; and the Academy of Finland.

^aVisiting scientists from

^bUniversity of Athens, 15784 Athens, Greece.

^cChinese Academy of Sciences, Beijing 100864, China.

^dUniversity of Bristol, Bristol BS8 1TL, United Kingdom.

^eUniversity Libre de Bruxelles, B-1050 Brussels, Belgium.

^fUniversity of California, Irvine, Irvine, CA 92697, USA.

^gUniversity of California, Santa Cruz, Santa Cruz, CA 95064, USA.

^hCornell University, Ithaca, NY 14853, USA.

ⁱUniversity of Cyprus, Nicosia CY-1678, Cyprus.

^jUniversity College Dublin, Dublin 4, Ireland.

^kUniversity of Edinburgh, Edinburgh EH9 3JZ, United Kingdom.

^lUniversity of Heidelberg, D-69120 Heidelberg, Germany.

^mUniversidad Iberoamericana, Mexico D.F., Mexico.

ⁿUniversity of Manchester, Manchester M13 9PL, England.

^oNagasaki Institute of Applied Science, Nagasaki, Japan.

^pUniversity de Oviedo, E-33007 Oviedo, Spain.

^qQueen Mary, University of London, London, E1 4NS, England.

^rTexas Tech University, Lubbock, TX 79409, USA.

^sIFIC (CSIC-Universitat de Valencia), 46071 Valencia, Spain.

- [1] A. Abulencia *et al.* (CDF Collaboration), Phys. Rev. Lett. **97**, 242003 (2006).
- [2] A. Lenz and U. Nierste, J. High Energy Phys. **06** (2007) 072.
- [3] I. Dunietz, R. Fleischer, and U. Nierste, Phys. Rev. D **63**, 114015 (2001).
- [4] R. Barate *et al.* (ALEPH Collaboration), Phys. Lett. B **486**, 286 (2000).
- [5] The charge conjugate state is implied throughout the paper. Our notation is such that, e.g., $B_s^0 \rightarrow D_s^-(\phi\pi^-)D_s^+(\phi\pi^+)$ refers to $B_s^0 \rightarrow D_s^-D_s^+$, followed by $D_s^- \rightarrow \phi\pi^-$ and $D_s^+ \rightarrow \phi\pi^+$, followed by $\phi \rightarrow K^+K^-$.
- [6] D. Acosta *et al.* (CDF Collaboration), Phys. Rev. D **71**, 032001 (2005).
- [7] CDF II uses a cylindrical coordinate system in which ϕ is the azimuthal angle, r is the radius from the symmetry axis, y points up, and z points in the proton beam direction with the origin at the center of the detector. The transverse plane is the plane perpendicular to the z axis.
- [8] A. Sill *et al.*, Nucl. Instrum. Methods Phys. Res., Sect. A **447**, 1 (2000).
- [9] T. Affolder *et al.*, Nucl. Instrum. Methods Phys. Res., Sect. A **526**, 249 (2004).
- [10] E.J. Thomson *et al.*, IEEE Trans. Nucl. Sci. **49**, 1063 (2002).
- [11] W. Ashmanskas *et al.*, Nucl. Instrum. Methods Phys. Res., Sect. A **518**, 532 (2004).
- [12] D. Langle, Nucl. Instrum. Methods Phys. Res., Sect. A **462**, 152 (2001).
- [13] E. Gershtein and M. Paulini, arXiv:physics/0306031.
- [14] G. Punzi, arXiv:physics/0308063.
- [15] W.-M. Yao *et al.*, J. Phys. G **33**, 1 (2006).
- [16] Frabetti *et al.* (FNAL E687 Collaboration), Phys. Lett. B **351**, 591 (1995).
- [17] P. Nason, S. Dawson, and R.K. Ellis, Nucl. Phys. B **303**, 607 (1988); **327**, 49 (1989).
- [18] D. Acosta *et al.* (CDF Collaboration), Phys. Rev. D **71**, 032001 (2005).